THE JOURNAL OF PHYSICAL CHEMISTRY A

Article

pubs.acs.org/JPCA

Infrared Photodissociation Spectroscopy of Mass Selected Homoleptic Copper Carbonyl Cluster Cations in the Gas Phase

Jieming Cui, Xiaojie Zhou, Guanjun Wang, Chaoxian Chi, Zhipan Liu,* and Mingfei Zhou*

Department of Chemistry, Shanghai Key Laboratory of Molecular Catalysts and Innovative Materials, Fudan University, Shanghai 200433, China

Supporting Information

ABSTRACT: Infrared spectra of mass-selected homoleptic copper carbonyl cluster cations including dinuclear $Cu_2(CO)_6^+$ and $Cu_2(CO)_7^+$, trinuclear $Cu_3(CO)_7^+$, $Cu_3(CO)_8^+$, and $Cu_3(CO)_9^+$, and tetranuclear $Cu_4(CO)_8^+$ are measured via infrared photodissociation spectroscopy in the carbonyl stretching frequency region. The structures are established by comparison of the experimental spectra with simulated spectra derived from density functional calculations. The $Cu_2(CO)_6^+$ cation is characterized to have an unbridged D_{3d} structure with a Cu−Cu half bond. The $Cu_2(CO)_7^+$ cation is determined to be a weakly bound complex involving a $Cu_2(CO)_6^+$ core ion. The trinuclear $Cu_3(CO)_7^+$ and $Cu_3(CO)_8^+$ cluster cations are determined to have triangle Cu_3 core structures with C_2 symmetry involving two $Cu(CO)_3$ groups and one $Cu(CO)_x$ group (x = 1 or 2). In contrast, the trinuclear $Cu_3(CO)_9^+$ cluster cation is determined to have an open chain-like $(OC)_3Cu–Cu(CO)_3–Cu(CO)_3$ structure. The tetranuclear $Cu_4(CO)_8^+$ cluster cation is characterized to have a tetrahedral Cu_4^+ core structure with all carbonyl groups terminally bonded.

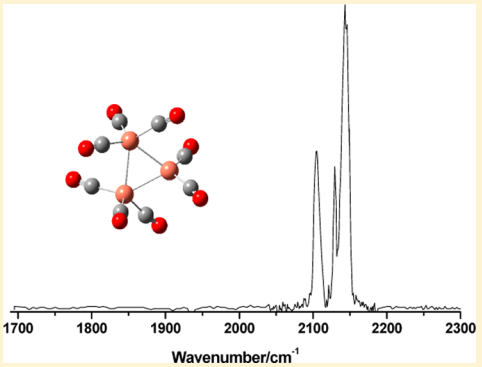

INTRODUCTION

Homoleptic transition metal carbonyls have been studied extensively because of their role in organometallic chemistry and catalysis.[1−4] Mononuclear copper carbonyl neutrals have been prepared in solid matrixes and were studied using infrared, UV−visible and electron spin resonance (ESR) spectroscopy.[5−14] Their structures and bonding have also been investigated with theory.[15−25] The dissociation energy of the CuCO complex was estimated via kinetic study in the gas phase.[26] The $Cu(CO)_n^+$ complexes have been studied in strongly acidic media, where the salts such as $[Cu(CO)_n]^+[Sb_2F_{11}]^-$ (n = 1−4) were synthesized and characterized using IR and Raman spectroscopy.[27−30] These studies indicated that the $Cu(CO)_n^+$ ions have blue-shifted CO frequencies. Copper carbonyl cations have also been studied in the gas phase, where the dissociation energies of $Cu(CO)_n^+$ (n = 1−4) species were measured.[31] The results show that up to four CO ligands are directly coordinated to the central copper ion. The $Cu(CO)_n^+$ (n = 1−4) cations as well as the $Cu(CO)_n^-$ (n = 1−3) anions have also been isolated and studied with infrared spectroscopy in rare gas matrixes.[14] Recently, infrared photodissociation spectroscopy in the carbonyl stretching frequency region is employed to study the small unsaturated complexes $Cu(CO)_n^+$ (n = 1−3) and the larger complexes at and beyond the filled coordination (n = 4−7).[32]

Compared to mononuclear copper carbonyls, multinuclear copper carbonyl clusters have received much less experimental and theoretical attention. Matrix isolation experiments show that the $Cu_2(CO)_n$ species were readily synthesized at very low temperatures.[6,9−12] Multinuclear Cu_nCO clusters with n = 1−4 were formed via the interaction of CO with small copper clusters and were identified spectroscopically in solid noble gas at cryogenic temperatures.[33] The reactivity of copper cluster cations, neutrals, and anions with CO has been studied in the gas phase, and the dissociation energies of small anionic copper clusters monocarbonyls (Cu_nCO^-, n = 3−7) were measured via the threshold collision-induced dissociation method.[34−38] The bonding of carbon monoxide to small copper clusters was theoretically studied.[39−51] Density functional theory calculations indicate that the optimal unsaturated $Cu_2(CO)_n$ (n = 1−6) structures are generated by joining 18-electron tetrahedral, 16-electron trigonal, 14-electron linear copper carbonyl building blocks, and/or bare copper atoms with copper−copper single bonds rather than by joining 18-electron copper carbonyl units with multiple copper−copper bonds.[52]

In the present article, homoleptic multinuclear copper carbonyl cluster cations are produced in the gas phase. The cations of interest are each mass-selected and studied by infrared photodissociation spectroscopy, a powerful method that has been successfully employed in studying transition metal carbonyl cations and anions in the gas phase.[53−73] The cluster structures are assigned by comparison of the

Received: May 28, 2013
Revised: July 24, 2013
Published: July 29, 2013

   dx.doi.org/10.1021/jp405250y | J. Phys. Chem. A 2013, 117, 7810−7817

experimental spectra with simulated spectra derived from density functional calculations.

EXPERIMENTAL AND COMPUTATIONAL METHODS

The infrared photodissociation spectra of the homoleptic copper carbonyl cluster cations were measured using a collinear tandem time-of-flight mass spectrometer. The experimental apparatus has been described in detail previously.[68] The cluster cations were produced in a Smalley-type laser vaporization supersonic cluster source. The 1064 nm fundamental of a Nd:YAG laser (Continuum, Minilite II, 10 Hz repetition rate and 6 ns pulse width) was used to vaporize a rotating copper metal target. The laser beam with 5−8 mJ/pulse is focused by a lens with a focal length of 300 mm. The copper carbonyl complexes were produced from the laser vaporization process in expansions of helium gas seeded with 4−6% CO using a pulsed valve (General Valve, Series 9) at 0.4−0.6 MPa backing pressure. After free expansion, the cations were skimmed and analyzed using a Wiley−McLaren time-of-flight mass spectrometer. The clusters of interest were each mass selected and decelerated into the extraction region of a second collinear time-of-flight mass spectrometer, where they were dissociated by a tunable IR laser. The fragment and parent cations were reaccelerated and mass analyzed by the second time-of-flight mass spectrometer.

The infrared source used in this study is generated by an KTP/KTA/AgGaSe2 optical parametric oscillator/amplifier system (OPO/OPA, Laser Vision) pumped by a Continuum Powerlite 8000 Nd:YAG laser, which is tunable from 800 to 5000 cm^{-1}, producing about 0.5−1.5 mJ/pulse in the range of 1600−2200 cm^{-1}. The infrared laser is loosely focused by a CaF_2 lens. The wavenumber of the OPO laser is calibrated using CO absorptions. The IR beam path is purged with nitrogen to minimize absorptions by air. Fragment ions and undissociated parent ions are detected by a dual microchannel plate detector. The ion signal is amplified, collected on a gated integrator, and averaged with a LabView based program. The photodissociation spectrum is obtained by monitoring the yield of the fragment ion of interest as a function of the dissociation IR laser wavelength and normalizing to parent ion signal. Typical spectra were recorded by scanning the dissociation laser in steps of 2 cm^{-1} and averaging over 250 laser shots at each wavelength.

Quantum chemistry calculations were performed to determine the molecular structures and to support the assignment of vibrational frequencies of the observed copper carbonyl cluster cations. Considering that there are many possible isomeric configurations of the copper carbonyl cluster cations, we have utilized the recently developed global optimization method, namely, the stochastic surface walking method (SSW) to search for the most stable isomers with the large-scale DFT calculations at the level of PBE functional.[74] The SSW method has demonstrated its ability for finding the global minimum of many challenging model potential systems, such as short-ranged Morse potential cluster and is particularly useful for treating molecular systems with special bonding motifs. In this work, our search starts from a few guessed structures and the search stops when no further stable structure appears after extensive runs. Typically, the most stable isomers will then be calculated using the hybrid B3LYP method in combination with the 6-31+G(d) basis set to confirm the relative energy sequence and to benchmark with the experimental IR spectrum. The B3LYP calculations were performed with the Gaussian 09 suite of quantum chemical software packages.[75] Theoretical predicted IR spectra were obtained by applying Lorentzian functions with the theoretical harmonic vibrational frequencies scaled by a factor of 0.9775 and a 7 cm^{-1} full width at half-maximum (fwhm). The scaling factor of 0.9775 was determined by calculating the average value needed to make the experimental and calculated frequencies coincide for the $Cu_n(CO)_m^+$ cluster cations studied.

RESULTS

The mass spectrum of copper carbonyl cluster cations produced by the laser vaporization supersonic cluster source in the m/z range of 100−550 is shown in Figure 1. The mass

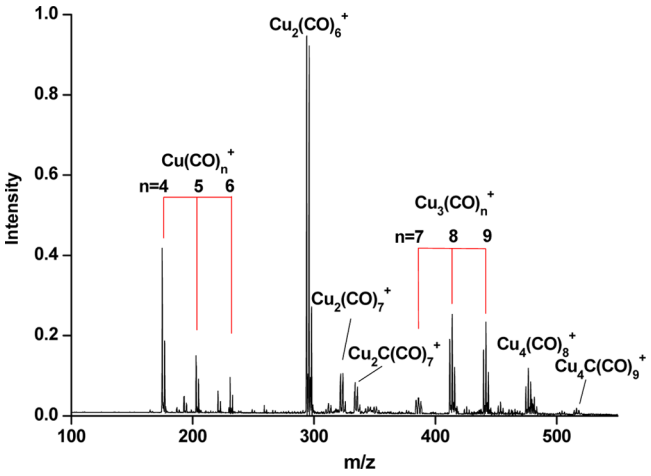

Figure 1. Mass spectrum of the copper carbonyl cluster cations produced by pulsed laser vaporization of a copper metal target in an expansion of helium seeded by carbon monoxide.

spectrum is composed of progressions of mass peaks due to mononuclear copper carbonyl cations $Cu(CO)_n^+$ (n = 4−6), dinuclear copper carbonyl cations $Cu_2(CO)_n^+$ (n = 6, 7), trinuclear carbonyl cations $Cu_3(CO)_n^+$ (n = 7−9), and tetranuclear carbonyl cluster cation $Cu_4(CO)_8^+$. Weak peaks due to $Cu_2C(CO)_7^+$ and $Cu_4C(CO)_9^+$ are also observed. For each species, the isotopic splitting of copper can clearly be resolved with their relative intensities matching the natural abundance isotopic distributions. The most abundant mononuclear cation $Cu(CO)_4^+$ has previously been characterized to have a completed coordination sphere with a tetrahedral structure similar to that of its neutral isoelectronic $Ni(CO)_4$, which satisfies the 18-electron rule.[32] The multinuclear carbonyl cluster cations of interest are each mass-selected and subjected to infrared photodissociation. When the IR laser is on a resonance with the CO stretching of the cluster cations, photofragmention of the cations via losing one or more CO ligand(s) takes place.

$Cu_2(CO)_6^+$. The $Cu_2(CO)_6^+$ cation dissociates via losing one CO ligand under focused IR laser irradiation with quite low efficiency. The parent ions can be depleted by about 8% at the laser pulse energy of about 1.1 mJ/pulse. The infrared photodissociation spectrum of $Cu_2(CO)_6^+$ in the 1700−2300 cm^{-1} region is shown in Figure 2. The spectrum exhibits a strong band centered at 2139 cm^{-1} together with a weak band centered at 2106 cm^{-1}. No bands below 2100 cm^{-1} were

dx.doi.org/10.1021/jp405250y | J. Phys. Chem. A 2013, 117, 7810−7817

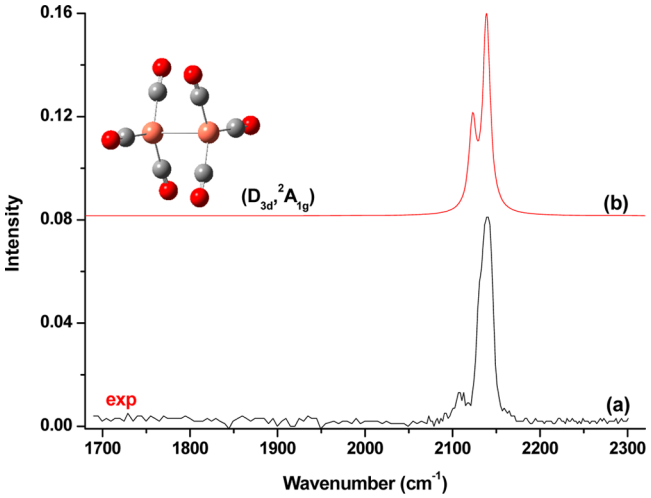

Figure 2. Experimental and simulated vibrational spectra of the $Cu_2(CO)_6^+$ cluster cation in the carbonyl stretching frequency region. The infrared photodissociation spectrum (a) was measured by monitoring the CO fragmentation channel leading to the formation of $Cu_2(CO)_5^+$. The simulated spectrum (b) was obtained from scaled harmonic vibrational frequencies and intensities for the D_{3d} structure calculated at the B3LYP/6-31+G(d) level.

observed, indicating that the CO ligands all are terminally bonded.

The $Cu_2(CO)_6^+$ cation was predicted to have a staggered D_{3d} structure with three terminally bonded carbonyls on each copper center. The eclipsed D_{3h} structure has a small imaginary frequency, which leads to the D_{3d} structure. The calculated infrared spectrum of the D_{3d} structure is shown in Figure 2b, which agrees well with the experimental spectrum. The observed and calculated band positions are compared in Table 1. The cation with D_{3d} symmetry has two IR active CO stretching vibrations. The experimentally observed 2106 cm^{-1} band is assigned to the A_{2u} stretching mode; while the 2139 cm^{-1} band is attributed to the doubly degenerate antisymmetric stretching vibration (E_u). These two modes of the cation are about 100 cm^{-1} higher than those of the $Cu_2(CO)_6$ neutral, which were observed at 2014 and 2035 cm^{-1} in adamantine and at 2003 and 2039 cm^{-1} in argon.[6,11,12]

$Cu_2(CO)_7^+$. The $Cu_2(CO)_7^+$ cation is also observed in the mass spectrum. It dissociates by losing one CO ligand very efficiently using an unfocused laser beam, indicating that the seventh CO is loosely bound. The parent ions can be depleted by more than 50%. The infrared photodissociation spectrum for the $Cu_2(CO)_7^+$ complex is shown in Figure 3. The spectrum exhibits four peaks centered at 2161, 2141, 2131, and 2107 cm^{-1}. The experimental observation suggests that no strongly bound seventh coordinated $Cu_2(CO)_7^+$ cation was produced in the experiments and that the observed $Cu_2(CO)_7^+$ cation is due to a weakly bound complex involving a $Cu_2(CO)_6^+$ core ion. The 2141, 2131, and 2107 cm^{-1} bands are originated from the $Cu_2(CO)_6^+$ core ion, which are very close to those of the $Cu_2(CO)_6^+$ cation. The 2161 cm^{-1} band can be attributed to the weakly bound external CO ligand. Previous studies have shown that the weakly bound external CO ligand(s) exhibits weak CO stretching vibration(s) in the range of 2160−2170 cm^{-1} for transition metal carbonyl cation complexes.[59−67] Using SSW global search method, we identified the two best isomers starting from different initial guess structures of $Cu_2(CO)_7^+$, as shown in Figure 3. The first structure is a

Table 1. Comparison of the Band Positions (in cm^{-1}) of the $Cu_m(CO)_n^+$ Cluster Cations Measured in the Present Work to Those Computed by Density Functional Theory at the B3LYP/6-31+G(d) level. (IR Intensities Are Listed in Parentheses in km/mol)

	exptl	calcd[a]
$Cu_2(CO)_6^+$	2106	2123 (1349)
		2131(0 × 2)
	2139	2139 (1546 × 2)
		2191 (0)
$Cu_2(CO)_7^+$	2107	2119 (1432)
	2131	2126 (97), 2127(85)
	2141	2136 (1489, 1471)
	2161	2181 (84),2189 (2)
$Cu_3(CO)_7^+$	2126	2118 (865), 2122 (441)
	2142	2136 (460),2136 (244)
	2146	2144 (1084)
	2162	2169 (529)
	2174	2188 (166)
$Cu_3(CO)_8^+$	2105	2103 (996), 2109 (347)
	2129	2128 (427), 2128 (109), 2135 (380)
	2143	2145 (1338), 2148 (1134)
		2179 (1)
$Cu_3(CO)_9^+$	2085	2063 (747, 745)
		2077 (0)
	2135	2137 (0), 2137 (10), 2139 (2742)
	2141	2141 (1437 × 2)
	2171	2181 (0)
$Cu_4(CO)_8^+$	2091	2096 (1499)
	2113	2102 (556), 2104 (304), 2106 (305), 2107 (1059)
	2121	2117 (1492)
	2137	2137 (1909)
	2159	2169 (32)

[a]The calculated harmonic vibrational frequencies were scaled by a factor of 0.9775.

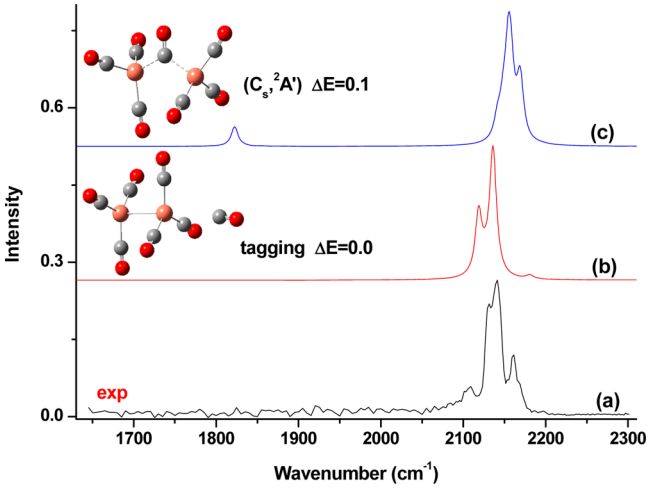

Figure 3. Experimental and simulated vibrational spectra of the $Cu_2(CO)_7^+$ cluster cation in the carbonyl stretching frequency region. The infrared photodissociation spectrum (a) was measured by monitoring the CO fragmentation channel leading to the formation of $Cu_2(CO)_6^+$. The simulated spectra (b,c) were obtained from scaled harmonic vibrational frequencies, and intensities for the two lowest-lying structures (the relative energies are listed in kcal/mol) calculated at the B3LYP/6-31+G(d) level.

dx.doi.org/10.1021/jp405250y | J. Phys. Chem. A 2013, 117, 7810−7817

weakly bound complex involving a $Cu_2(CO)_6^+$ core ion with its predicted spectrum (Figure 3b) in agreement with the experiment. Another structure has C_s symmetry with one bridging CO ligand. These two structures have essentially the same energy. The C_s structure was predicted to have a bridge bonded CO stretching vibration in the 1800 cm^{-1} region (Figure 3c). Apparently, no such band was observed in the experimental spectrum of $Cu_2(CO)_7^+$.

$Cu_3(CO)_7^+$. The $Cu_3(CO)_7^+$ cluster cation has a low signal intensity in the mass spectrum. It dissociates quite efficiently via the loss of one CO fragment with low laser energy, the resulting infrared photodissociation spectrum is shown in Figure 4. The

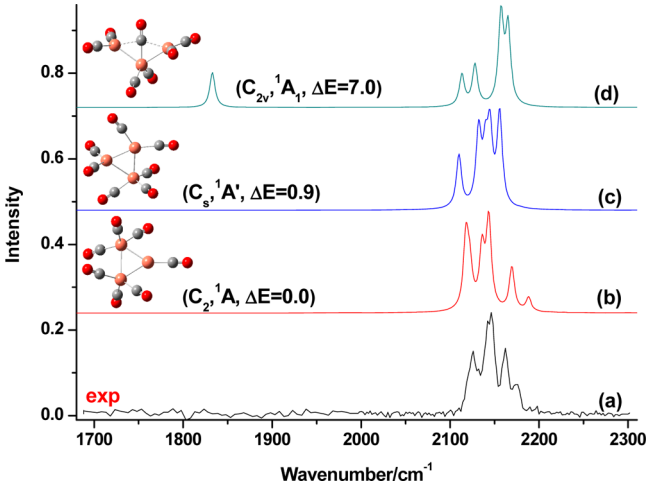

Figure 4. Experimental and simulated vibrational spectra of the $Cu_3(CO)_7^+$ cluster cation in the carbonyl stretching frequency region. The infrared photodissociation spectrum (a) was measured by monitoring the CO fragmentation channel leading to the formation of $Cu_3(CO)_6^+$. The simulated spectra (b–d) were obtained from scaled harmonic vibrational frequencies, and intensities for the three lowest energy structures (the relative energies are listed in kcal/mol) calculated at the B3LYP/6-31+G(d) level.

spectrum exhibits four well-resolved bands centered at 2126, 2146, 2162, and 2174 cm^{-1} together with a partially resolved shoulder at 2142 cm^{-1}. No bands below 2100 cm^{-1} were observed, indicating that the CO ligands all are terminally bonded. Using SSW global search method, we identified three lowest energy isomers starting from different initial guess structures of $Cu_3(CO)_7^+$ and their structures are shown in Figure 4. The most stable structure has C_2 symmetry involving a triangle Cu_3 core with all of the carbonyl groups terminally bonded. The axial copper center is coordinated by one terminal CO unit, while the other two copper centers are each coordinated by three terminal CO units. The second lowest-energy isomer also involves a triangle Cu_3 ring with one $Cu(CO)_3$ unit and two $Cu(CO)_2$ units with C_s symmetry. This isomer lies above the global minimum structure by only 0.9 kcal/mol. The third isomer has an open chain structure $(OC)_2Cu–Cu(CO)_3–Cu(CO)_2$ with C_{2v} symmetry. This structure was predicted to lie above the global minimum by 7.0 kcal/mol. The calculated infrared spectra are compared to the experimental one in Figure 4. Only the calculated spectrum of the lowest energy isomer matches with the experiment.

$Cu_3(CO)_8^+$. The $Cu_3(CO)_8^+$ cluster cation has a relatively large signal intensity in the mass spectrum. It dissociates quite efficiently via loss of one CO fragment with low laser energy. The infrared photodissociation spectrum is shown in Figure 5. The spectrum exhibits only three bands centered at 2105, 2129,

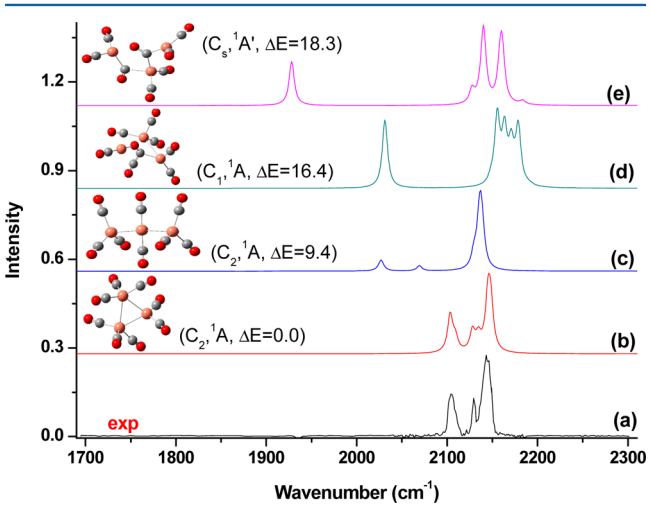

Figure 5. Experimental and simulated vibrational spectra of the $Cu_3(CO)_8^+$ cluster cation in the carbonyl stretching frequency region. The infrared photodissociation spectrum (a) was measured by monitoring the CO fragmentation channel leading to the formation of $Cu_3(CO)_7^+$. The simulated spectra (b–e) were obtained from scaled harmonic vibrational frequencies, and intensities for the four lowest energy structures (the relative energies are listed in kcal/mol) calculated at the B3LYP/6-31+G(d) level.

and 2143 cm^{-1}. The four lowest lying structures obtained from theory are shown in Figure 5. The most stable structure involves a triangle Cu_3 core with C_2 symmetry. In this structure, the axial copper center is coordinated by two terminal CO units, while the other two copper centers are each coordinated by three terminal CO units. This structure can be regarded as being derived from the most stable structure of $Cu_3(CO)_7^+$ by adding a CO group to the CuCO fragment. The second lowest-energy isomer involves an open chain $(OC)_3Cu–Cu(CO)_2–Cu(CO)_3$ structure with C_2 symmetry. This isomer lies above the global minimum structure by 9.4 kcal/mol. The third and the fourth isomers both have open chain structures and were predicted to lie more than 15 kcal/mol above the global minimum structure. The calculated infrared spectra of these four structures of $Cu_3(CO)_8^+$ are compared to the experimental spectrum in Figure 5. Only the lowest energy structure matches well with the experiment.

$Cu_3(CO)_9^+$. The $Cu_3(CO)_9^+$ cation is able to lose up to two CO units quite efficiently. The IR spectrum obtained by monitoring the loss of one CO fragment is shown in Figure 6. The spectrum recorded via the loss of two CO ligands is essentially the same as that of one CO loss channel. Three bands centered at 2085, 2145, and 2171 cm^{-1} can clearly be resolved. In addition, a band at 2135 cm^{-1} can also be partially resolved in the spectrum. In contrast to $Cu_3(CO)_7^+$ and $Cu_3(CO)_8^+$, which were characterized to have triangle Cu_3 structures, the $Cu_3(CO)_9^+$ cation was predicted to have an open chain-like $(OC)_3Cu–Cu(CO)_3–Cu(CO)_3^+$ structure (Figure 6) with each copper center coordinated by three terminal CO ligands. The Cu_3 chain is almost linear. Another structural isomer involving a triangle Cu_3 core with each copper coordinated by three terminal CO units with C_s symmetry was predicted to be 5.1 kcal/mol less stable than the open chain-like structure. The calculated infrared spectra of these two

dx.doi.org/10.1021/jp405250y | J. Phys. Chem. A 2013, 117, 7810–7817

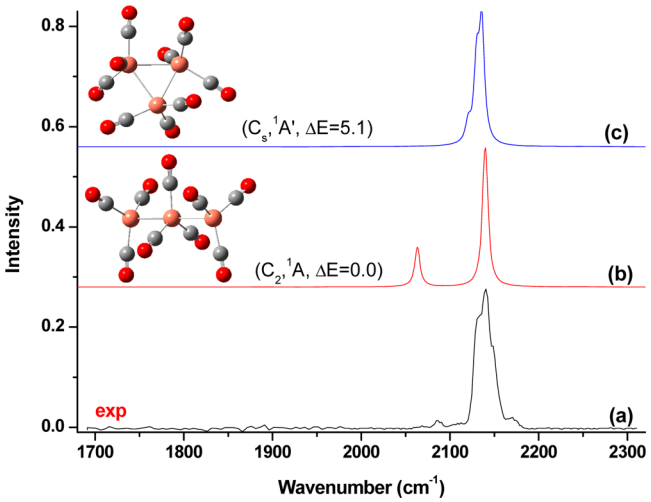

Figure 6. Experimental and simulated vibrational spectra of the $Cu_3(CO)_9^+$ cluster cation in the carbonyl stretching frequency region. The infrared photodissociation spectrum (a) was measured by monitoring the CO fragmentation channel leading to the formation of $Cu_3(CO)_8^+$. The simulated spectra (b,c) were obtained from scaled harmonic vibrational frequencies, and intensities for the two lowest energy structures (the relative energies are listed in kcal/mol) calculated at the B3LYP/6-31+G(d) level.

structures are compared to the experimental spectrum in Figure 6. The more stable open chain structure matches better than the less stable cyclic structure.

$Cu_4(CO)_8^+$. The $Cu_4(CO)_8^+$ cluster cation is the only tetranuclear carbonyl species observed in the mass spectrum shown in Figure 1. The cation is able to lose one and two CO ligand(s). The infrared photodissociation spectrum of $Cu_4(CO)_8^+$ consists of four bands centered at 2091, 2121, 2137, and 2159 cm^{-1} (Figure 7). In addition, a weak band at 2113 cm^{-1} can be partially resolved. Apparently, this cation also involves only terminally bonded CO ligands since no bands

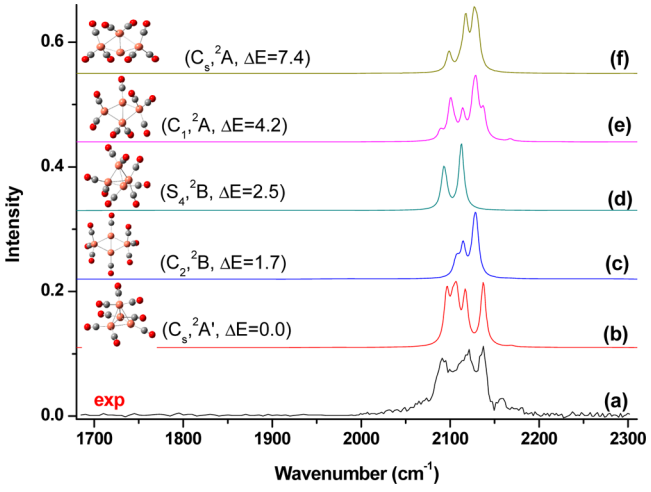

Figure 7. Experimental and simulated vibrational spectra of the $Cu_4(CO)_8^+$ cluster cation in the carbonyl stretching frequency region. The infrared photodissociation spectrum (a) was measured by monitoring the CO fragmentation channel leading to the formation of $Cu_4(CO)_7^+$. The simulated spectra (b–f) were obtained from scaled harmonic vibrational frequencies, and intensities for the five lowest energy structures (the relative energies are listed in kcal/mol) calculated at the B3LYP/6-31+G(d) level.

below 2000 cm^{-1} were observed. The five lowest lying structures obtained from theory are shown in Figure 7. The global minimum structure of $Cu_4(CO)_8^+$ is found to have C_s symmetry involving a tetrahedral Cu_4 core (Figure 7). In this structure, one copper center is coordinated by three CO ligands, two copper atoms are each coordinated by two CO ligands, and the fourth copper atom is coordinated by one CO ligand. The third lowest lying structure (2.5 kcal/mol higher in energy) also involves a tetrahedral Cu_4 core. In this structure, each copper center is coordinated by two CO ligands with S_4 symmetry. The other three structures all involve a rhombus Cu_4 core, which lie about 1.7, 4.2, and 7.4 kcal/mol higher in energy than the most stable isomer. The calculated infrared spectra of the five lowest energy structures of $Cu_4(CO)_8^+$ are compared to the experimental spectrum in Figure 7. The calculated spectrum of the lowest energy C_s structure provides the best match with the experiment.

DISCUSSION

The features observed in the mass spectrum recorded in the present experiments provide some valuable information on the maximum number of CO molecules (saturation limits) that bind to small copper cluster cations. Previous studies indicate that the $Cu(CO)_4^+$ cation has a completed coordination sphere with a tetrahedral structure similar to that of its neutral isoelectronic analogue $Ni(CO)_4$.[32] Thus, the Cu^+ cation has a coordination number of four toward CO. Although the $Cu_2(CO)_7^+$ cation is the largest dinuclear cluster complex observed in the mass spectrum, it was characterized to be a weakly bound complex involving a $Cu_2(CO)_6^+$ core ion. Thus, the $Cu_2(CO)_6^+$ cation is the coordination saturated cluster. The $Cu_2(CO)_6$ neutral was previously observed in solid matrixes, which was regarded as s coordination saturated neutral cluster.[6,11,12] Previous theoretical studies indicate that the eclipsed and staggered ethane-like structures for neutral $Cu_2(CO)_6$ are virtually degenerate and lie significantly lower in energy than other possible structures. The eclipsed Cu–Cu bond distance is predicted to be 2.61 Å, while that for the staggered structure is 2.65 Å. In both structures, the Cu–Cu bond is a single bond to satisfy the 18-electron rule.[52] The Cu–Cu bond length of the $Cu_2(CO)_6^+$ cation is predicted to be 2.897 Å, more than 0.2 Å longer than those of the neutral structures. This bond length is also significantly longer than that of Cu_2^+ with a $^2\Sigma_g$ ground state.[76] Natural bond orbital (NBO) analysis indicates that only one valence molecular orbital is involved in the Cu–Cu bonding. This orbital is formed by two 4s atomic orbitals of copper and is σ bonding (Figure. 8). This orbital is singly occupied. Therefore, the Cu–Cu bond can be regarded as a half bond with both copper centers exhibiting 17 valence electrons. Recent investigation indicates that the Ni_2^+ cation coordinates eight CO ligands in forming the $Ni_2(CO)_8^+$ cation, which was characterized to have a symmetric D_{3d} structure with a Ni–Ni half bond.[73]

The Cu_3^+ cluster cation is found to be able to coordinate up to nine CO ligands. The $Cu_3(CO)_7^+$, $Cu_3(CO)_8^+$, and $Cu_3(CO)_9^+$ cluster cations are presented in the mass spectrum. The $Cu_3(CO)_7^+$ and $Cu_3(CO)_8^+$ cluster cations are determined to have a triangle Cu_3 core with C_2 symmetry. In contrast, the experimentally observed $Cu_3(CO)_9^+$ cluster cation is characterized to have an open chain-like structure. These observations indicate that $Cu_3(CO)_9^+$ is the saturation level for linear Cu_3^+, while $Cu_3(CO)_8^+$ is the saturation level for cyclic Cu_3^+. Adding a CO ligand to $Cu_3(CO)_8^+$ leading to $Cu_3(CO)_9^+$ results in the

dx.doi.org/10.1021/jp405250y | J. Phys. Chem. A 2013, 117, 7810–7817

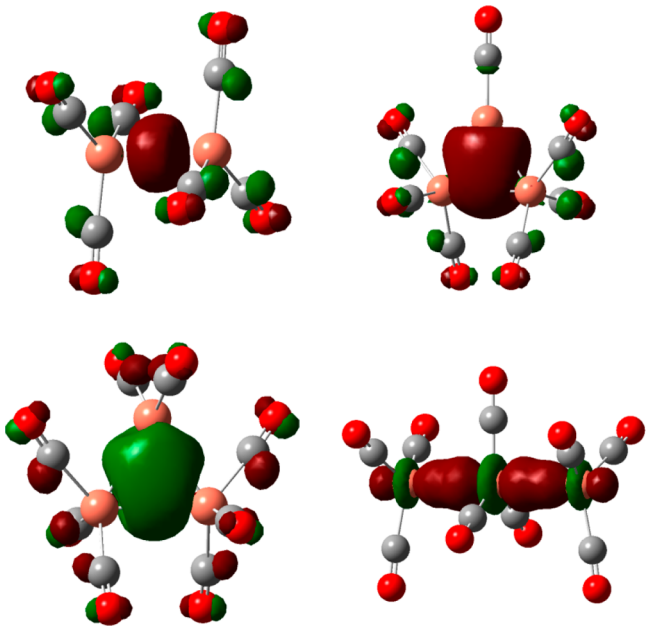

Figure 8. Bonding orbitals related to the Cu−Cu bonds in $Cu_2(CO)_6^+$, $Cu_3(CO)_7^+$, $Cu_3(CO)_8^+$, and $Cu_3(CO)_9^+$.

opening of the triangle Cu_3 to linear chain. The (OC)Cu−$Cu(CO)_3$ and $(OC)_3Cu-Cu(CO)_3$ bond distances in $Cu_3(CO)_7^+$ are predicted to be 2.511 and 2.754 Å, respectively. The $(OC)_2Cu-Cu(CO)_3$ and $(OC)_3Cu-Cu(CO)_3$ bond distances in $Cu_3(CO)_8^+$ are 2.610 and 2.732 Å, respectively. Both $Cu_3(CO)_7^+$ and $Cu_3(CO)_8^+$ can be regarded as being formed via the interactions of the CO ligands with the ground state Cu_3^+ cation, which has an $^1A_1'$ ground state with cyclic D_{3h} symmetry.[76] As has been pointed out previously, the contribution of the d electrons is small; therefore, the bonding of cyclic Cu_3^+ can roughly be regarded as involving only a 3c−2e σ bond formed by three 4s atomic orbitals of copper (Figure 8).[76] Natural population analysis indicates that the positive charge is almost evenly distributed on the three $Cu(CO)_n$ subunits in $Cu_3(CO)_7^+$ and $Cu_3(CO)_8^+$. The $Cu_3(CO)_9^+$ cluster cation with a linear Cu_3 core can be regarded as being formed via the interactions of the CO ligands with the linear $^1\Sigma_g$ state of Cu_3^+, which was predicted to be about 1.5 eV less stable than the cyclic Cu_3^+ isomer.[76] The linear $^1\Sigma_g$ state of Cu_3^+ also involves a 3c−2e σ bond, the Cu−Cu bonds both can be regarded as half bonds (Figure 8). Therefore, the central copper has an 18 formal valence electron configuration, while the two terminal copper centers have only 17 valence electrons. Consistent with the above notion, natural population analysis indicates that the positive charge is evenly distributed on the two terminal $Cu(CO)_3$ subunits with the central $Cu(CO)_3$ subunit being almost neutral.

The $Cu_4(CO)_8^+$ cluster cation is the only tetranuclear carbonyl cluster cation observed in the mass spectrum shown in Figure 1, suggesting that the saturation limit of CO coordination on Cu_4^+ is eight. The observed $Cu_4(CO)_8^+$ cluster cation is characterized to have C_s symmetry with a tetrahedral Cu_4 core. Previous theoretical studies indicate that the most stable Cu_4^+ cation has a D_{2h} rhombus structure with a $^2B_{3u}$ ground state. The tetrahedron structure in a $^2T_2$ state was predicted to be slightly higher in energy than the rhombus structure.[76] The $Cu_4(CO)_8^+$ cluster cation can be regarded as being formed via the interactions of the CO ligands with the tetrahedral Cu_4^+ cation in the $^2T_2$ state.

CONCLUSIONS

Homoleptic multinuclear copper carbonyl cluster cations are produced in a laser vaporization supersonic cluster source in the gas phase. The cluster cations of interest are each mass-selected and studied by infrared photodissociation spectroscopy in the carbonyl stretching frequency region. The structures are established by comparison of the experimental spectra with simulated spectra derived from density functional calculations. The $Cu_2(CO)_6^+$ cation is determined to be the coordination saturated cluster, which is characterized to have an unbridged D_{3d} structure with a Cu−Cu half bond. The $Cu_2(CO)_7^+$ cation is determined to be a weakly bound complex involving a $Cu_2(CO)_6^+$ core ion. The $Cu_3(CO)_7^+$ and $Cu_3(CO)_8^+$ cluster cations are determined to have triangle Cu_3 core structures with C_2 symmetry involving two $Cu(CO)_3$ groups and one $Cu(CO)_x$ group (x = 1 or 2). Both cluster cations can be regarded as being formed via the interactions of the CO ligands with the $^1A_1'$ ground state cyclic Cu_3^+ cation. In contrast, the $Cu_3(CO)_9^+$ cluster cation is determined to have an open chain-like $(OC)_3Cu-Cu(CO)_3-Cu(CO)_3$ structure. The $Cu_3(CO)_9^+$ cluster cation with a linear Cu_3 core can be regarded as being formed via the interactions of the CO ligands with the linear $^1\Sigma_g$ state of Cu_3^+. The $Cu_4(CO)_8^+$ cluster cation is the only tetranuclear carbonyl cluster cation observed, suggesting that the saturation limit of CO coordination on Cu_4^+ is eight. It is characterized to have a tetrahedral Cu_4^+ core structure with all carbonyl groups terminally bonded.

ASSOCIATED CONTENT

Supporting Information

Calculated geometries, vibrational frequencies and intensities, and complete ref 75. This material is available free of charge via the Internet at http://pubs.acs.org.

AUTHOR INFORMATION

Corresponding Author

*Fax: (+86) 21-6564-3532. E-mail: mfzhou@fudan.edu.cn (M.Z.); zpliu@fudan.edu.cn (Z.L.).

Notes

The authors declare no competing financial interest.

ACKNOWLEDGMENTS

We gratefully acknowledge financial support from National Natural Science Foundation (Grant No. 20933030, 21273045, and 21173053), Ministry of Science and Technology of China (2013CB834603, 2010CB732306, and 2012YQ220113-3), and the Committee of Science and Technology of Shanghai (13XD1400800).

REFERENCES

(1) Cotton, F. A.; Wilkinson, G.; Murillo, C. A.; Bochmann, M. *Advanced Inorganic Chemistry*, 6th ed.; John Wiley: New York, 1999.

(2) Cotton, F. A.; Walton, R. A. *Multiple Bonds Between Metal Atoms*; Clarendon Press: Oxford, U.K., 1993.

(3) Housecroft, C. E. *Metal−Metal Bonded Carbonyl Dimers and Clusters*; Oxford University Press: Oxford, U.K., 1996.

(4) Zhou, M. F.; Andrews, L.; Bauschlicher, C. W., Jr. Spectroscopic and Theoretical Investigations of Vibrational Frequencies in Binary Unsaturated Transition-Metal Carbonyl Cations, Neutrals, and Anions. *Chem. Rev.* **2001**, *101*, 1931−1961.

(5) Ogden, J. S. Infrared Spectroscopic Evidence for Copper and Silver Carbonyls. *J. Chem. Soc. D: Chem. Commun.* **1971**, *16*, 978−979.
(6) Huber, H.; Kundig, E. P.; Moskovits, M.; Ozin, G. A. Binary Copper Carbonyls: Synthesis and Characterization of $Cu(CO)_3$, $Cu(CO)_2$, CuCO and $Cu_2(CO)_6$. *J. Am. Chem. Soc.* **1975**, *97*, 2097−2106.
(7) Kasai, P. H.; Jones, P. M. Copper Carbonyls, CuCO and $Cu(CO)_3$: Matrix-Isolation Electron Spin Resonance Study. *J. Am. Chem. Soc.* **1985**, *107*, 813−818.
(8) Xu, Q.; Jiang, L. Oxidation of Carbon Monoxide on Group 11 Metal Atoms: Matrix-Isolation Infrared Spectroscopic and Density Functional Theory Study. *J. Phys. Chem. A* **2006**, *110*, 2655−2662.
(9) Howard, J. A.; Mile, B.; Morton, J. R.; Preston, K. F. EPR Spectra of Copper(0) and Silver(0) Tricarbonyls and Tricyanides. *J. Phys. Chem.* **1986**, *90*, 2027−2029.
(10) Howard, J. A.; Mile, B.; Morton, J. R.; Preston, K. F.; Sutcliffe, R. Electron Paramagnetic Resonance Spectrum of Copper Tricarbonyl ($Cu(CO)_3$): An Inorganic Isolobal Analog of Methyl. *J. Phys. Chem.* **1986**, *90*, 1033−1036.
(11) Chenier, J. H. B.; Hampson, C. A.; Howard, J. A.; Mile, B. A Spectroscopic Study of the Reaction of Cu Atoms with CO in a Rotating Cryostat: Evidence for the Formation of CuCO, $Cu(CO)_3$ and $Cu_2(CO)_6$. *J. Phys. Chem.* **1989**, *93*, 114−117.
(12) Mile, B.; Howard, J. A.; Tomietto, M.; Joly, H. A.; Sayari, A. Preparation of Small Copper Particles of High Catalytic Activity Using a Rotating Cryostat. *J. Mater. Sci.* **1996**, *31*, 3073−3080.
(13) Tremblay, B.; Manceron, L. Far-Infrared Spectrum and Structure of Copper Monocarbonyl Isolated in Solid Argon. *Chem. Phys.* **1999**, *242*, 235−240.
(14) Zhou, M. F.; Andrews, L. Infrared Spectra and Density Functional Calculations of $Cu(CO)_n^+$ (n = 1−4), $Cu(CO)_n$ (n = 1−3), and $Cu(CO)_n^-$ (n = 1−3), in Solid Neon. *J. Chem. Phys.* **1999**, *111*, 4548−4557.
(15) Arratia-Perez, R.; Axe, F. U.; Marynick, D. S. Geometry, Bonding and Optical and Magnetic Properties of Copper Tricarbonyl: A Theoretical Study. *J. Phys. Chem.* **1987**, *91*, 5177−5183.
(16) Berthier, G.; Daoudi, A.; Suard, M. Electronic Structure and Bonding of Transition Metal Complexes MCO (M = Cu, Fe, Ti). *J. Mol. Struct.* **1988**, *179*, 407−415.
(17) Pilme, J.; Silvi, B.; Alikhani, M. S. Structure and Stability of M−CO, M = First Transition Row Metal: An Application of Density Functional Theory and Topological Approaches. *J. Phys. Chem. A* **2003**, *107*, 4506−4514.
(18) Bauschlicher, C. W.; Bagus, P. S.; Nelin, C. J.; Roos, B. O. The Nature of the Bonding in XCO for X = Fe, Ni, and Cu. *J. Chem. Phys.* **1986**, *85*, 354−364.
(19) Lupinetti, A. J.; Jonas, V.; Thiel, W.; Strauss, S. H.; Frenking, G. Trends in Molecular Geometries and Bond Strengths of the Homoleptic d^{10} Metal Carbonyl Cations $[M(CO)_n]^{x+}$(M^{x+} = Cu^+, Ag^+, Au^+, Zn^{2+}, Cd^{2+}, Hg^{2+}; n=1−6): A Theoretical Study. *Chem.—Eur. J.* **1999**, *5*, 2573−2583.
(20) Merchan, M.; Nebotgil, I.; Gonzalezluque, R.; Orti, E. A CI Study of the CuCO and $CuCO^+$ Complexes. *J. Chem. Phys.* **1987**, *87*, 1690−1700.
(21) Fournier, R. Theoretical Study of Linear and Bent CrCO, NiCO and CuCO. *J. Chem. Phys.* **1993**, *98*, 8041−8050.
(22) Fournier, R. Theoretical Study of the Monocarbonyls of First Row Transition Metal Atoms. *J. Chem. Phys.* **1993**, *99*, 1801−1815.
(23) Bauschlicher, C. W., Jr. An ab Initio Study of CuCO. *J. Chem. Phys.* **1994**, *100*, 1215−1218.
(24) Barone, V. Structure, Thermochemistry and Magnetic Properties of Binary Copper Carbonyls by a Density Functional Approach. *J. Phys. Chem.* **1995**, *99*, 11659−11666.
(25) Wu, G. S.; Li, Y. W.; Xiang, H. W.; Xu, Y. Y.; Sun, Y. H.; Jiao, H. J. Density Functional Investigation on Copper Carbonyl Complexes. *J. Mol. Struct.* **2003**, *637*, 101−107.
(26) Blitz, M. A.; Mitchell, S. A.; Hackett, P. A. Gas Phase Reactions of Copper Atoms: Formation of $Cu(CO)_2$, $Cu(C_2H_2)_2$ and $Cu(C_2H_4)_2$. *J. Phys. Chem.* **1991**, *95*, 8719−8726.
(27) Souma, Y.; Iyoda, J.; Sano, H. Formation and Properties of Group 1B Metal Carbonyl Cations. *Inorg. Chem.* **1976**, *15*, 968−970.
(28) Rack, J. J.; Webb, J. D.; Strauss, S. H. Polycarbonyl Cations of Cu(I), Ag(I), and Au(I): $[M(CO)_n]^+$. *Inorg. Chem.* **1997**, *36*, 99−106.
(29) Strauss, S. H. Copper(I) and Silver(I) Carbonyls. To Be or Not to Be Nonclassical. *J. Chem. Soc., Dalton Trans.* **2000**, *1*, 1−6.
(30) Ivanova, S. M.; Ivanov, S. V.; Miller, S. M.; Anderson, O. P.; Solntsev, K. A.; Strauss, S. H. Mono-, Di-, Tri-, and Tetracarbonyls of Copper(I), Including the Structures of $Cu(CO)_2$(1-Bn-$CB_{11}F_{11}$) and $[Cu(CO)_4]$[1-Et-$CB_{11}F_{11}$]. *Inorg. Chem.* **1999**, *38*, 3756−3757.
(31) Meyer, F.; Chen, Y. M.; Armentrout, P. B. Sequential Bond Energies of $Cu(CO)_x^+$ and $Ag(CO)_x^+$ (x = 1−4). *J. Am. Chem. Soc.* **1995**, *117*, 4071−4081.
(32) Brathwaite, A. D.; Reed, Z. D.; Duncan, M. A. Infrared Photodissociation Spectroscopy of Copper Carbonyl Cations. *J. Phys. Chem. A* **2011**, *115*, 10461−10469.
(33) Moskovits, M.; Hulse, J. E. The lnteraction of CO with Very Small Copper Clusters. *J. Phys. Chem.* **1977**, *81*, 2004−2009.
(34) Lian, L.; Akhtar, F.; Hackett, P. A.; Rayner, D. M. Reactions of the Copper Dimer, Cu_2, in the Gas Phase. *Int. J. Chem. Kinet.* **1994**, *26*, 85−96.
(35) Leuchtner, R. E.; Harms, A. C.; Castleman, A. W., Jr. Metal Cluster Cation Reactions: Carbon Monoxide Association to Cu_n^+ Ions. *J. Chem. Phys.* **1990**, *92*, 6527−6537.
(36) Holmgren, L.; Gronbeck, H.; Andersson, M.; Rosen, A. CO on Copper Clusters: Orbital Symmetry Rules. *Phys. Rev. B* **1996**, *53*, 16644−16651.
(37) Lee, T. H.; Ervin, K. M. Reactions of Copper Group Cluster Anions with Oxygen and Carbon Monoxide. *J. Phys. Chem.* **1994**, *98*, 10023−10031.
(38) Spasov, V. A.; Lee, T. H.; Ervin, K. M. Threshold Collision-Induced Dissociation of Anionic Copper Clusters and Copper Cluster Monocarbonyls. *J. Chem. Phys.* **2000**, *112*, 1713−1720.
(39) Boussard, P. J. E.; Siegbahn, P. E. M.; Svensson, M. The Interaction of Ammonia, Carbonyl, Ethylene and Water with the Copper and Silver Dimers. *Chem. Phys. Lett.* **1994**, *231*, 337−344.
(40) Nygren, M. A.; Siegbahn, P. E. M. Theoretical Study of Chemisorptions of CO on Copper Clusters. *J. Phys. Chem.* **1992**, *96*, 7579−7584.
(41) Fournier, R. Theoretical Study of the Bonding of Ammonia, Carbon Monoxide and Ethylene to Copper Atom, Dimer and Trimer. *J. Chem. Phys.* **1995**, *102*, 5396−5407.
(42) Rochefort, A.; Fournier, R. Quantum Chemical Study of CO and NO Bonding to Pd_2, Cu_2, and PdCu. *J. Phys. Chem.* **1996**, *100*, 13506−13513.
(43) Hirabayashi, S.; Ichihashi, M.; Kawazoe, Y.; Kondow, T. Comparison of Adsorption Probabilities of O_2 and CO on Copper Cluster Cations and Anions. *J. Phys. Chem. A* **2012**, *116*, 8799−8806.
(44) Cao, Z. X.; Wang, Y. J.; Zhu, J.; Wu, W.; Zhang, Q. N. Static Polarizabilities of Copper Cluster Monocarbonyls Cu_nCO (n = 2−13) and Selectivity of CO Adsorption on Copper Clusters. *J. Phys. Chem. B* **2002**, *106*, 9649−9654.
(45) Post, D.; Baerends, E. J. Cluster Studies of CO Adsorption. III. CO on Small Cu Clusters. *J. Chem. Phys.* **1983**, *78*, 5663−5681.
(46) Sosa1, R. M.; Gardiol, P. Electronic Structure and Properties of MCO and M_5CO Carbonyls (M = Fe, Ni, Cu) by Density Functional Methods. *Int. J. Quantum Chem.* **1996**, *60*, 1429−1441.
(47) Poater, A.; Duran, M.; Jaque, P.; Toro-Labbe, A.; Sola, M. Molecular Structure and Bonding of Copper Cluster Monocarbonyls Cu_nCO (n = 1−9). *J. Phys. Chem. B* **2006**, *110*, 6526−6536.
(48) Nygren, M. A.; Siegbahn, P. E. M. Electronic Shell Closings in Metal Cluster Plus Adsorbate Systems: Cu_7^+CO and Cu_{17}^+CO. *J. Chern. Phys.* **1991**, *95*, 6181−6184.
(49) Jiang, L.; Xu, Q. Theoretical Study of the Interaction of Carbon Monoxide with 3d Metal Dimmers. *J. Chem. Phys.* **2008**, *128*, 124317.
(50) Pike, R. D. Structure and Bonding in Copper(I) Carbonyl and Cyanide Complexes. *Organometallics* **2012**, *31*, 7647−7660.

(51) Padilla-Campos, L. Theoretical Study of the Adsorption of Carbon Monoxide on Small Copper Clusters. *J. Mol. Struct.* **2008**, *851*, 15−21.
(52) Li, Q. S.; Liu, Y. D.; Xie, Y. M.; King, R. B.; Schaefer, H. F. Binuclear Homoleptic Copper Carbonyls $Cu_2(CO)_x$ (x = 1−6): Remarkable Structures Contrasting Metal−Metal Multiple Bonding with Low-Dimensional Copper Bonding Manifolds. *Inorg. Chem.* **2001**, *40*, 5842−5850.
(53) Lemaire, J.; Boissel, P.; Heninger, M.; Mauclaire, G.; Bellec, G.; Mestdagh, H.; Simon, A.; Caer, S. L.; Ortega, J. M.; Glotin, F.; Maitre, P. Gas Phase Infrared Spectroscopy of Selectively Prepared Ions. *Phys. Rev. Lett.* **2002**, *89*, 273002.
(54) Fielicke, A.; von Helden, G.; Meijer, G.; Pedersen, D. B.; Simard, B.; Rayner, D. M. Size and Charge Effects on the Binding of CO to Small Isolated Rhodium Clusters. *J. Phys. Chem. B* **2004**, *108*, 14591−14598.
(55) Fielicke, A.; von Helden, G.; Meijer, G.; Pedersen, D. B.; Simard, B.; Rayner, D. M. Size and Charge Effects on the Binding of CO to Late Transition Metal Clusters. *J. Chem. Phys.* **2006**, *124*, 194305.
(56) Fielicke, A.; von Helden, G.; Meijer, G.; Simard, B.; Rayner, D. M. Gold Cluster Carbonyls: Vibrational Spectroscopy of the Anions and the Effects of Cluster Size, Charge, and Coverage on the CO Stretching Frequency. *J. Phys. Chem. B* **2005**, *109*, 23935−23940.
(57) Fielicke, A.; von Helden, G.; Meijer, G.; Pedersen, D. B.; Simard, B.; Rayner, D. M. Gold Cluster Carbonyls: Saturated Adsorption of CO on Gold Cluster Cations, Vibrational Spectroscopy, and Implications for Their Structures. *J. Am. Chem. Soc.* **2005**, *127*, 8416−8423.
(58) Moore, D. T.; Oomens, J.; Eyler, J. R.; Meijer, G.; von Helden, G.; Ridge, D. P. Gas-Phase IR Spectroscopy of Anionic Iron Carbonyl Clusters. *J. Am. Chem. Soc.* **2004**, *126*, 14726−14727.
(59) Ricks, A. M.; Reed, Z. D.; Duncan, M. A. Infrared Spectroscopy of Mass-Selected Metal Carbonyl Cations. *J. Mol. Spectrosc.* **2011**, *266*, 63−74.
(60) Velasquez, J., III; Duncan, M. A. IR Photodissociation Spectroscopy of Gas Phase $Pt^+(CO)_n$ (n = 4−6). *Chem. Phys. Lett.* **2008**, *461*, 28−32.
(61) Velasquez, J., III; Njegic, B.; Gordon, M. S.; Duncan, M. A. IR Photodissociation Spectroscopy and Theory of $Au^+(CO)_n$ Complexes: Nonclassical Carbonyls in the Gas Phase. *J. Phys. Chem. A* **2008**, *112*, 1907−1913.
(62) Ricks, A. M.; Bakker, J. M.; Douberly, G. E.; Duncan, M. A. Infrared Spectroscopy and Structures of Cobalt Carbonyl Cations, $Co(CO)_n^+$ (n = 1−9). *J. Phys. Chem. A* **2009**, *113*, 4701−4708.
(63) Reed, Z. D.; Duncan, M. A. Infrared Spectroscopy and Structures of Manganese Carbonyl Cations, $Mn(CO)_n^+$ (n = 1−9). *J. Am. Soc. Mass Spectrom.* **2010**, *21*, 739−749.
(64) Ricks, A. M.; Reed, Z. D.; Duncan, M. A. Seven-Coordinate Homoleptic Metal Carbonyls in the Gas Phase. *J. Am. Chem. Soc.* **2009**, *131*, 9176−9177.
(65) Ricks, A. M.; Gagliardi, L.; Duncan, M. A. Infrared Spectroscopy of Extreme Coordination: The Carbonyls of U^+ and UO_2. *J. Am. Chem. Soc.* **2010**, *132*, 15905−15907.
(66) Chi, C. X.; Cui, J. M.; Li, Z. H.; Xing, X. P.; Wang, G. J.; Zhou, M. F. Infrared Photodissociation Spectra of Mass Selected Homoleptic Dinuclear Iron Carbonyl Cluster Anions in the Gas Phase. *Chem. Sci.* **2012**, *3*, 1698−1706.
(67) Wang, G. J.; Cui, J. M.; Chi, C. X.; Zhou, X. J.; Li, Z. H.; Xing, X. P.; Zhou, M. F. Bonding in Homoleptic Iron Carbonyl Cluster Cations: A Combined Infrared Photodissociation Spectroscopic and Theoretical Study. *Chem. Sci.* **2012**, *3*, 3272−3279.
(68) Wang, G. J.; Chi, C. X.; Cui, J. M.; Xing, X. P.; Zhou, M. F. Infrared Photodissociation Spectroscopy of Mononuclear Iron Carbonyl Anions. *J. Phys. Chem. A* **2012**, *116*, 2484−2489.
(69) Chi, C. X.; Cui, J. M.; Xing, X. P.; Wang, G. J.; Liu, Z. P.; Zhou, M. F. Infrared Photodissociation Spectroscopy of Trigonal Bipyramidal 19-Electron $Ni(CO)_5^+$ Cation. *Chem. Phys. Lett.* **2012**, *542*, 33−36.
(70) Cui, J. M.; Xing, X. P.; Chi, C. X.; Wang, G. J.; Liu, Z. P.; Zhou, M. F. Infrared Photodissociation Spectra of Mass-Selected Homoleptic Dinuclear Palladium Carbonyl Cluster Cations in the Gas Phase. *Chin. J. Chem.* **2012**, *30*, 2131−2137.
(71) Zhou, X. J.; Cui, J. M.; Li, Z. H.; Wang, G. J.; Zhou, M. F. Infrared Photodissociation Spectroscopic and Theoretical Study of Homoleptic Dinuclear Chromium Carbonyl Cluster Cations with a Linear Bridging Carbonyl Group. *J. Phys. Chem. A* **2012**, *116*, 12349−12356.
(72) Zhou, X. J.; Cui, J. M.; Li, Z. H.; Wang, G. J.; Liu, Z. P.; Zhou, M. F. Carbonyl Bonding on Oxophilic Metal Centers: Infrared Photodissociation Spectroscopy of Mononuclear and Dinuclear Titanium Carbonyl Cation Complexes. *J. Phys. Chem. A* **2013**, *117*, 1514−1521.
(73) Cui, J. M.; Wang, G. J.; Zhou, X. J.; Chi, C. X.; Li, Z. H.; Liu, Z. P.; Zhou, M. F. Infrared Photodissociation Spectra of Mass Selected Homoleptic Nickel Carbonyl Cluster Cations in the Gas Phase. *Phys. Chem. Chem. Phys.* **2013**, *15*, 10224−10232.
(74) Shang, C.; Liu, Z. P. Stochastic Surface Walking Method for Structure Prediction and Pathway Searching. *J. Chem. Theory Comput.* **2013**, *9*, 1838−1845.
(75) Frisch, M. J.; Trucks, G. W.; Schlegel, H. B.; Scuseria, G. E.; Robb, M. A.; Cheeseman, G.; Scalmani, J. R.; Barone, V.; Mennucci, B.; Petersson, G. A.; et al. *Gaussian 09*, revision A.2; Gaussian, Inc.: Wallingford, CT, 2009.
(76) Calaminici, P.; Koster, A. M.; Russo, N.; Salahub, D. R. A Density Functional Study of Small Copper Clusters: Cu_n ($n \leq 5$). *J. Chem. Phys.* **1996**, *105*, 9546−9556.